Multiple time scales analysis of runoff series based on the Chaos Theory

Xinjie Li[a,b,*], Guoming Gao[a], Tiesong Hu[b], Huaibao Ma[a], Tao Li[a]

[a]*Center for Yellow River Xiaolangdi Research, Yellow River Institute of Hydraulic Research,
Zhengzhou 450003, China*
Email: xin_wd@163.com
[b]*School of Water Resources and Hydropower Engineering, Wuhan University, Wuhan 430072, China*

ABSTRACT

The significance of accepting runoff processes as nonlinear has been gaining considerable in recent times. However, it is hard to explore the types of nonlinearity acting underlying the runoff processes and the intensity of the nonlinearity at different timescales. Daily runoff time series observed at the Pingshan hydrometric station are used for this study. An attempt is made to identify the existence of chaos and the intensity of nonlinear behavior at three characteristic time scales (one day, 1/3 month, and one month). Six nonlinear dynamic methods are used: (1) phase space reconstruction and the delay time is estimated using average mutual information; (2) the sufficient embedding dimension is estimated using the false nearest neighbor algorithm; (3) correlation dimension method; (4) Lyapunov exponent method; (5) 0–1 test algorithm for chaos; and (6) the multi-step Volterra adaptive method. A comparison of results reveals the presence of low-dimensional chaos in the runoff dynamics at the various time scales and the time scales composes only a limit fraction of the intensity of nonlinear behavior. The reasonably good predictions indicate the efficiency of the nonlinear prediction method for predicting the runoff series.

Keywords: Chaos; Correlation dimension; Lyapunov exponent; Volterra adaptive method

1. Introduction

Estimating runoff plays an important role in modeling towards decision-making related to the process of development of water resources, management of river basins, estimation of risk, and preventing floods and droughts [1]. However, runoff processes are taken as continuous processes; hydrologic data-sets are discrete time series. Suffered by data sample length, subjectivity of parameter selection, and noise of runoff series, thus a host of associated uncertainties in modeling and forecasting is its sensitivity to the infinitesimal changes in its initial conditions [2]. The existence of low-dimensional chaos is likely to stem from the initiation of a combination of catchment processes, such as uneven distribution of rainfall in seasonal variation, tributary inputs in different river

*Corresponding author.

area, and saturation of groundwater flows [3]. Most of the research in literature confirms the presence of chaos in the runoff time series [4]. Nonetheless, the existence of low-dimensional chaos has been a topic in wide dispute. Because on one hand, there is no common knowledge about what type of nonlinearity exists in the runoff process, and on the other hand, it is not clear how the character and intensity of nonlinearity of runoff processes changes as the timescale changes [5].

It is hard to explore different types of nonlinearity one by one which may possibly act underlying runoff processes. We here want to investigate the existence of general nonlinearity in the runoff process from an unvaried time series data based quantitative point of view. There are a wide variety of methods available presently to test linearity or nonlinearity, which may be divided into two categories: the model-driven approaches which are based on the phase space reconstruction, such as the correlation dimension method, the largest Lyapunov exponent, and Kolmogorov entropy method. The other method is the data-driven approaches, such as artificial neural network [6] and 0–1 test algorithm [7–9]. Hydrological processes in river catchments are subject to well-known seasonal variations, river basin area, the existence of climatic patterns in rainfall processes, and the collective impact of such a wide range of deterministic and stochastic factors, the nonlinearity of the runoff time series become more and more uncertainty [10].

With these observations, this paper investigates the existence of chaotic behavior in the runoff time series from Jinsha River basin, China. Runoff data observed over a period of 53 years (1940–1992) are studied at different timescales. Six nonlinear dynamic methods, with varying levels of complexity, are employed: (1) phase space reconstruction; (2) correlation dimension method; (3) false nearest neighbor (FNN) algorithm; (4) Lyapunov exponent method; (5) 0–1 test algorithm for chaos; and (6) the multi-step Volterra adaptive method. These methods provide either direct or indirect identification of chaotic behaviors. A key feature of this study is the investigation of possible interference of chaotic behaviors at different timescales.

2. Chaos identification methods

For chaos characteristics is the inherent reflection of system variables in the time interval [11], so the characteristics of time series is the inner reflect through the external sequence. In the present study, an attempt is made to identify chaos using various techniques by generating ensembles in order to quantify the uncertainty involved. The analysis was based on widely used nonlinear dynamic methods: (1) average mutual information to determine the delay time and reconstruct phase space; (2) false nearest neighbor algorithm and correlation dimension method to estimate the dimensionality; (3) Lyaponov exponent methods and the multi-step Volterra adaptive method to investigate convergence/ divergence and predictability; and (4) 0–1 test algorithm for quantitative analysis.

2.1. Phase space reconstruction

Among a variety of methods available for reconstructing the phase space, the most popular one is the method of delays. The method was proposed by Packard et al. and was introduced and mathematically demonstrated by Takens [12]. The method is based on the concept that, using its past history and an appropriate delay time, a scalar time series can be reconstructed in a multi-dimensional phase space to represent the underlying dynamics. According to this approach, if appropriate embedding dimension m and delay time τ are chosen, the dynamics can be fully embedded in m-dimensional phase space represented by the vector:

$$Y_i = (x_i, x_{i+\tau}, \ldots, x_{i+(m-1)\tau})^T \tag{1}$$

where τ is referred to as the delay time and for a digitized time series is a multiple of the sampling interval used, $i = 1, 2,\ldots, N - (m-1)\tau/\Delta t$; m is termed the embedding dimension; and Δt is the sampling time.

A variety of techniques have emerged for detecting the existence of chaos. For instance, the popular methods used for estimating the delay time τ are: (1) autocorrelation function method (ACF); (2) the average mutual information method (AMI); and (3) correlation integral (CI). ACF method only reflects linear characteristics of the time sequence, CI method need more data. For study of hydrological time series, the most popularly used method is the AMI method [13].

AMI as an information theoretic technique suggested by Kantz and Schreiber, are estimated for different lag time to estimate the approximate embedding dimensions. Since autocorrelations only measure linear dependence, mutual information provides an enhanced nonlinear estimate of the time lag for use in the phase space reconstruction. The AMI method defines how the measurements X_t at time t are connected in an information theoretic fashion to measurements $X_{t+\tau}$ at time $t + \tau$.

The average mutual information is commonly computed in the form as given below:

$$\text{AMI}(\tau) = \sum_{x_i, x_{i-\tau}} p(x_i, x_{i-\tau}) \log\left[\frac{p(x_i, x_{i-\tau})}{p(x_i)p(x_{i-\tau})}\right] \quad (2)$$

where $\text{AMI}(\tau)$ is the mutual information of two discrete variables x_i and $x_{i-\tau}$, $p(x_i)$, and $p(x_{i-\tau})$ are the individual probability of x_i and $x_{i-\tau}$, respectively. $p(x_i, x_{i-\tau})$ is the joint probability density of x_i and $x_{i-\tau}$. Conversely, a lower value of $\text{AMI}(\tau)$ means a lower interrelationship between the two measurement x_i and $x_{i-\tau}$. One frequently used to select the first local minimum of AMI between two measurements x_i and $x_{i-\tau}$ as the time delay.

2.2. Estimation of system dimensionality

The embedding dimension m is usually determined using the FNN method. When the percentage of these false nearest neighbors drops to zero, the geometric structure of the attractor has been unfolded and the orbits of the system are now distinct and do not cross.

Correlation dimension is one of the most efficient nonlinear measures of the correlation between pairs lying on the attractor. If the correlation dimension gets a finite fractional value even on increase in embedding dimension m, then the time series under investigation is generally considered as chaotic on the other hand, it is stochastic.

The correlation dimension method is also known as correlation integral analysis which is estimated by the G-P algorithm. According to the reconstructed phase space of the vector (1), the correlation integral function $C(r)$ is given by:

$$C(r) = \lim_{N\to\infty} \frac{1}{N(N-1)} \sum_{i,j=1}^{N} H(r - |Y_i - Y_j|), \; i \neq j \quad (3)$$

where N is the number of data; H is the Heaviside step function, with $H(u)=1$ for $u \geqslant 0$, and $H(u)=0$ for $u \leqslant 0$, where $u = r - |Y_i - Y_j|$; r is the radius of sphere centered on Y_i or Y_j, for small values of r, the correlation function $C(r)$ is related to the radius r by the following relation: $C(r) \sim r^{D2}$, where D_2 is the correlation exponent, which can be calculated from the slope of the $log C(r)$ versus $log r$ in plot given by:

$$D_2 = \lim_{r\to\infty} \log C(r) / \log r \quad (4)$$

If the correlation exponent D_2 increases without saturation value with increasing embedding dimension m, then the time series is generally considered to be stochastic series. On the contrary, if the correlation exponent D_2 saturates to a constant value on increase in embedding dimension m, the time series is generally considered to be chaotic.

The FNN algorithm was introduced by Kennel et al. and provides information on the optimal embedding dimension of the phase space for representing the system dynamics. After a short time into the future, the percentage of these false nearest neighboring states would drops to zero. The geometric orbits of the attractor have been extended out and the trajectory of the system does not intersect and are distinct. The basic idea in the false nearest neighbor algorithm is to determine how to decide upon increasing the embedding dimension that a nearest neighbor is false. In this study, the false nearest neighbor method is implemented using the TISEAN package and is used to determine the minimal sufficient embedding dimension m of the series.

2.3. Lyapunov exponents

The largest Lyapunov exponent is another indicator to determine the presence of chaotic behavior [14]. It gives the averaged divergence information of nearby trajectories in the phase space. A positive Lyapunov exponent indicates an exponential divergence of the nearby trajectories, and is a strong indicator of chaos. There are many algorithms to calculate the maximal Lyapunov exponent. Rosenstein et al. [15] proposed the small data-sets method to calculate the maximal Lyapunov exponent from an observed time series because it takes advantage of all the available data. For an observed time series, choosing appropriate embedding dimension m and delay time τ, the phase space is reconstructed. A point $x(n_0)$ is chosen and all the points $x(n_0)$ with the diameter are selected, and the average distance between them is calculated. An average quantity S is calculated by repeating for N number of points along the orbit, which is known as the stretching factor:

$$S = \frac{1}{N} \sum_{n_0} \ln \frac{1}{u_{x(n_0)}} |x(n_0) - x(n)| \quad (5)$$

where $|u_{x(n0)}|$ is the number of neighbors found around point $x(n_0)$. If S exhibits a linear increase, then its slope can be taken as an estimate of the largest lyapunov exponent λ. So the largest Lyapunov exponent λ is defined as:

$$\lambda_1 = \frac{1}{t_M - t_0} \sum_{k=1}^{M} \log_2 \frac{L'(t_k)}{L(t_{k-1})} \quad (6)$$

where $L(t_k)$ is the Euclidean distance, and M is the number of iteration, $L'(t_k)$ is referred to the evolution length of $L(t_k)$ when the time is given as $T = t_k$.

2.4. The multi-step Volterra adaptive method

The essence of the time series prediction is an inverse problem of dynamic system, that is, given an observed scalar sequence the system dynamics model could be reconstructed as following:

$$x(t' + T) = f(x(t), x(t + \tau), ..., x(t + (m + 1)\tau)) \qquad (7)$$

where $t' = t+(m-1)\tau$, T is forward prediction step length. Due to a large number of nonlinear system can be expressed by Volterra series, Volterra series can be interpreted in the nonlinear approximation function F(•), so the filter of series prediction is:

$$x(n + 1) = h_0 + \sum_{k=1}^{p} y_k(n) \qquad (8)$$

$$y_k(n) = \sum_{i_1,...,i_k=0}^{m-1} h_k(i_1, ..., i_k) \prod_{j=1}^{k} x(n - i_j \tau) \qquad (9)$$

where p is the order of the filter; h_k $(i_1,...,i_k)$ is the nuclear to the order p. In practical applications, the prediction of low-dimensional chaotic time series the coupling structure is done based on the three-order Volterra filter.

2.5. Principle of the 0–1 test algorithm for chaos

The numerical algorithm for chaotic identification is proposed by Gottwald[8]. Given a one-dimensional discrete observable data-set $\varphi(n)$ at time $n = 1,2,..., N$. Choose a parameter c at random between 0 and 2π, one defines:

$$p_c = \sum_{j=1}^{n} \varphi(j) \cos(\theta(j)), \quad n = 1, 2, ..., N \qquad (10)$$

$$q_c = \sum_{j=1}^{n} \varphi(j) \sin(\theta(j)), \quad n = 1, 2, ..., N \qquad (11)$$

$$\theta(j) = jc + \sum_{i=1}^{j} \varphi(i), \quad j = 1, 2, ..., N \qquad (12)$$

The mean-square displacement is defined as:

$$M(n) = M_c(n) - (E(\phi))^2((1 - \cos nc)/(1 - \cos c)) \qquad (13)$$

$$M_c = \lim_{N \to \infty} \frac{1}{N} \sum_{j=1}^{N} [(p(j + n) - p(j))^2 - (q(j + n) - q(j))^2] \qquad (14)$$

$$E(\varphi) = \lim_{N \to \infty} \frac{1}{N} \sum_{j=1}^{N} \varphi(j) \qquad (15)$$

The asymptotic growth rate K_c is given by the definition:

$$K_c = \lim_{n \to \infty} \log D_c(n) / \log n \qquad (16)$$

If the behavior of p vs. q is Brownian, $M(n)$ grows linearly in time, then $K_c \approx 1$, the underlying characteristic of data-set $\varphi(n)$ is chaotic. If the behavior of p vs. q is bounder, $M(n)$ is a bounded function in time, $K_c \approx 0$; the underlying characteristic of data-set $\varphi(n)$ is non-chaotic. The test is now that K_c close to zero means regular dynamics and K_c close to 1 implies chaotic dynamics. Based on the above parameters, the method provides a simple visual test method whether the underlying characteristic of data-set $\varphi(n)$ is chaotic or nonchaotic.

3. Case study

The daily runoff data of Pingshan hydrological station on the Jinsha River in China are considered for the present study [16]. The length of its trunk is 2,316 km, and the drainage area is 0.34 million km². Over the territory rich in water resources, many hydropower stations and dams have been built across the river. The observed daily runoff data is 53 years (19,359 days) long with an observation period from January 1940 to December 1992. The daily time series
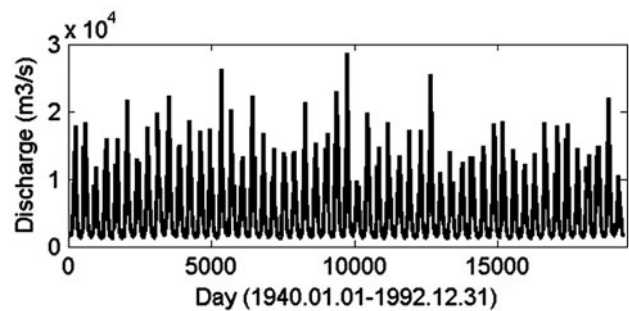

Fig. 1. Time series plot for river in Pingshan hydrological station.

Table 1
The statistical parameters of runoff data of Pinshan hydrologic Station at different timescales

Statistics	Number	Min (m³/s)	Max (m³/s)	Average (m³/s)	Standard-D	Skew	Kurtosis
Daily	19,359	1,060	28,600	4,575	3948.55	1.4427	1.8395
1/3 month	1908	9,090	239,800	46,421	39,529	1.3227	1.2367
month	636	33,340	582,500	139,263	113,347	1.1122	0.3291

graph is given in Fig. 1. Monthly series are obtained from daily data by taking average of daily discharges in every month. The statistical characteristics of the runoff series at different timescales are summarized in Table 1.

3.1. Phase space

The reconstruction of phase space diagram for runoff time series at different timescale are shown in Fig. 2. There is an attractor in the phase space, which is reconstructed in two dimensions ($m = 2$) with delay time $t = 1$, the $\{x_i, x_{i+1}\}$ state-space maps with different timescale are displayed in Fig. 2. For both time series, the phase space diagram exhibit clear attractors in well-defined regions, suggesting that dynamic characteristics of the system are simple and can possibly are indicated by deterministic chaos, without a need for stochastic modeling.

The delay time is commonly selected by using the mutual information method where the function first attains a minimum. The runoff data are used for chaotic nature analysis and for determining delay time. As a preliminary investigation, the mutual information function of the three runoff series are plotted and shown in Fig. 3. Day 96 is selected as the time delay of the daily runoff data of 53 years, because this observation is the first local minimum observed from Fig. 3 (left). Thus, the time delay of 13 is selected as the time delay of the 1/3 monthly runoff data of 53 years from Fig. 3 (right). The 5 month is selected as the month runoff data of 53 year from Fig. 3 (lower). The initial exponential decay of mutual information

functions indicates that the runoff series may be of chaotic nature. The periodic behavior of the mutual information for higher lags is due to the seasonal periodicity of the rainfall.

3.2. Dimension estimation

The FNN method provides a further evidence for the presence of low-order chaos in the time series for the present study. It is implemented by varying the values of the embedded dimension from 1 to higher values until the percentage of these false nearest neighbors drops to zero. The results in Fig. 4 show that the value of embedding dimension is 8, 6, and 5, respectively. The identification of these values means that both time series have an attractor, the geometric structure of which is unfolded as a distinct system whose orbits are distinct and do not cross.

To further verify the reliability of the best delay time, this paper has selected the correlation dimension method. We calculated the correlation function for our data-set using the delay times ($\tau = 96$, 13, 5), determined by the mutual information method in the previous section, with the embedding dimension m increases gradually from 1 to 20, the log C(r) versus log r graphs and the correlation exponent v versus log r for the three runoff series are shown in Figs. 5 and 6, respectively. It can be seen that the correlation exponent value increases with the embedding dimension up to a certain value and then saturates beyond that value. The saturation of the correlation exponent beyond a certain embedding dimension value is an indication of the existence of deterministic dynamics.
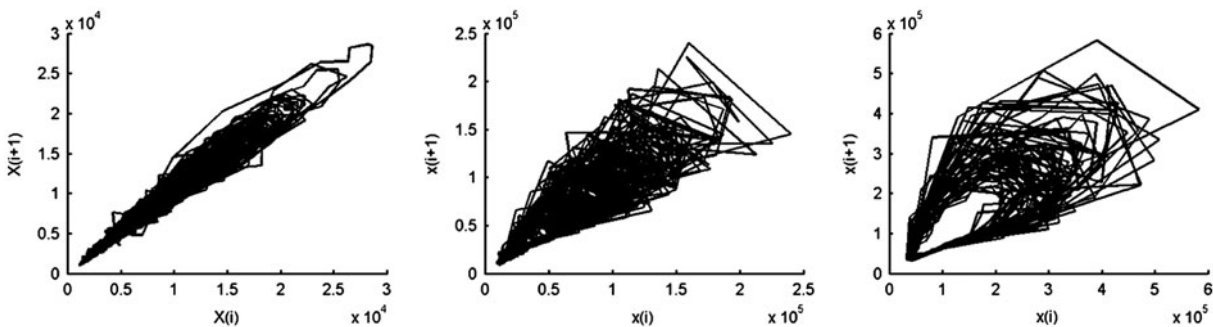

Fig. 2. Phase space maps; left: daily runoff series; right: 1/3 monthly runoff series; and lower: monthly runoff series.
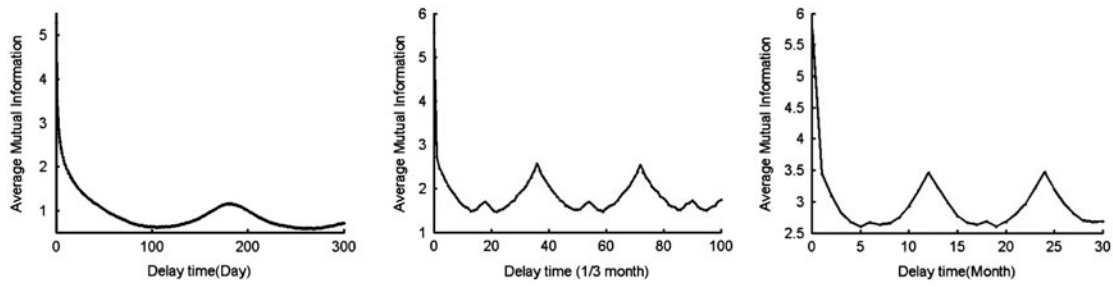
Fig. 3. Average mutual information; left: daily runoff series; right: 1/3 monthly runoff series; and lower: monthly runoff series.
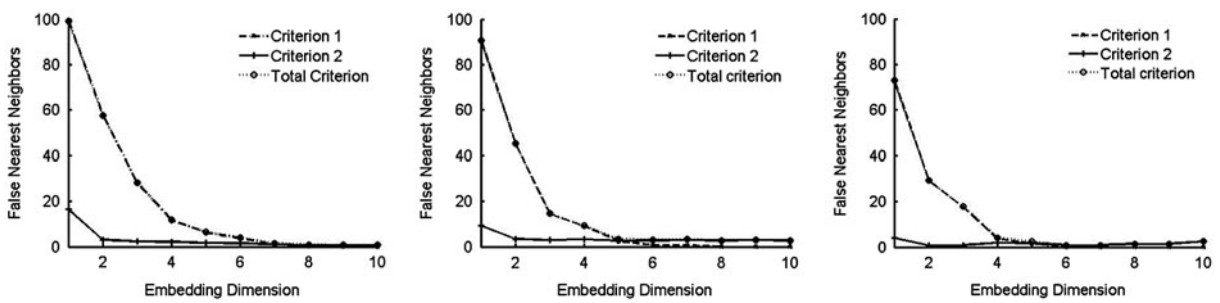

Fig. 4. False nearest neighbors; left: daily runoff series; right: 1/3 monthly runoff series; and lower: monthly runoff series.
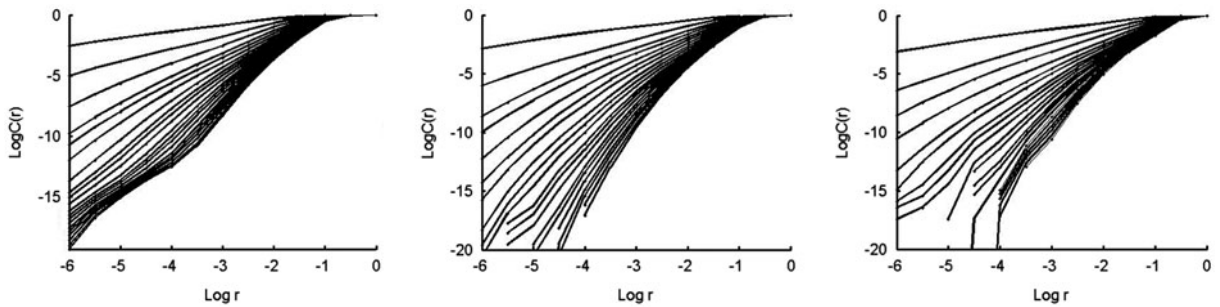

Fig. 5. log $C(r)$~log r plot; left: daily runoff series; right: 1/3 monthly runoff series; and lower: monthly runoff series.
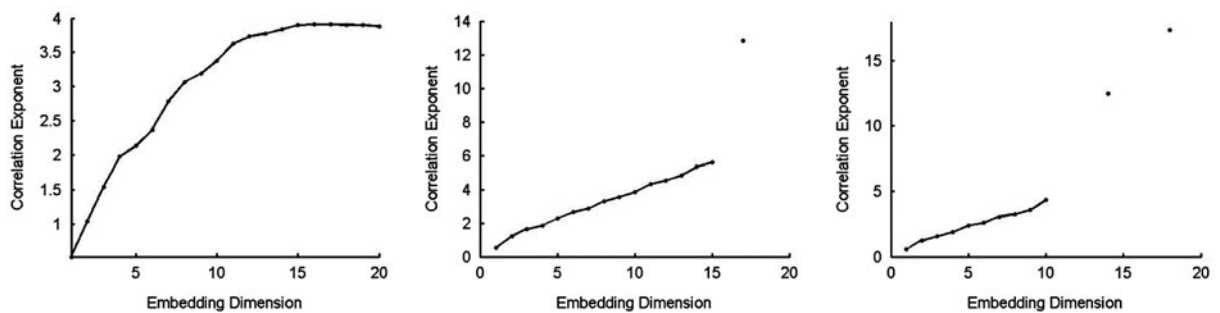

Fig. 6. Correlation integral results; left: daily runoff series; right: 1/3 monthly runoff series; and lower: monthly runoff series.

The saturated correlation dimension of the two runoff series are about $d_1 = 3.957$, $d_2 = 5.7$, and $d_3 = 4.35$, respectively. The saturated value of correlation dimension suggests the possible presence of chaotic behavior in the three runoff time series.

3.3. Lyapunov exponent method

Using the optimal delay time and embedding dimension as before. The largest Lyapunov exponent could be calculated by the small amount data method. Fig. 7 shows the curves for the stretching factors vs. the number of points N indicating an expected linear increase leading towards flat regions with some fluctuations superimposed on the linear part of the curve. The slope vales corresponding to the largest Lyapunov exponents are obtained after the least squares line fitted for different timescale time series with the respective values being 0.0018, 0.0034, and 0.0077.

3.4. The multi-step Volterra adaptive method

The runoff series of different time series are normalized and then the normalized samples are used to train the Volterra series. The calculation of the method is simple because it has only two parameters with a certain leading time. Because, the seasonality in the raw flow series play a role in nonlinearity. As the timescale increases, the nonlinearity weakens, and the effects of seasonal variance dominate the nonlinearity of some 1/3 monthly and monthly runoff series. It has been shown in runoff series that the multi-step Volterra method brings bad prediction effect at the peak in which this method has poor hydrocarbon prediction effect in Fig. 8. It is shown that the result of model calculation is very close to the measured data, and that further forecast on the tendency of the equipment condition could possibly be made by this method. Prediction performance will drop with the lapse of time. Melt temperature had no influence on the hollow ratio when the temperature reached a specific range. This prediction results also indicated that there exists some weak nonlinearity in daily, 1/3 monthly, and monthly series of Jinsha River.

3.5. The 0–1 test algorithm

To demonstrate the reliability and universality of the test, we apply the 0–1 test algorithm to above three runoff series. The plots of asymptotic growth rate are shown in Fig. 9.

The length of the runoff series affects the nonlinear of runoff sequence. When the length of the runoff series increases, the asymptotic growth rate of runoff series K_c increase gradually, runoff series that periodic gradually abate. It is noted that, the nonlinearity
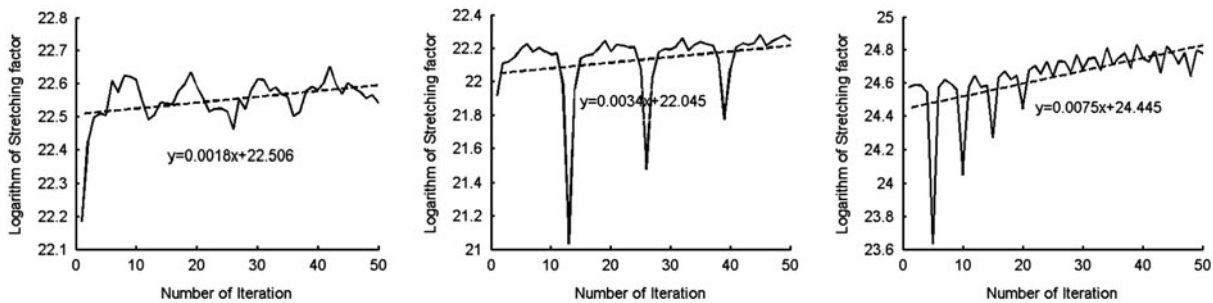

Fig. 7. Lyapunov exponents; Left: daily runoff series; right: 1/3 monthly runoff series; lower: monthly runoff series.
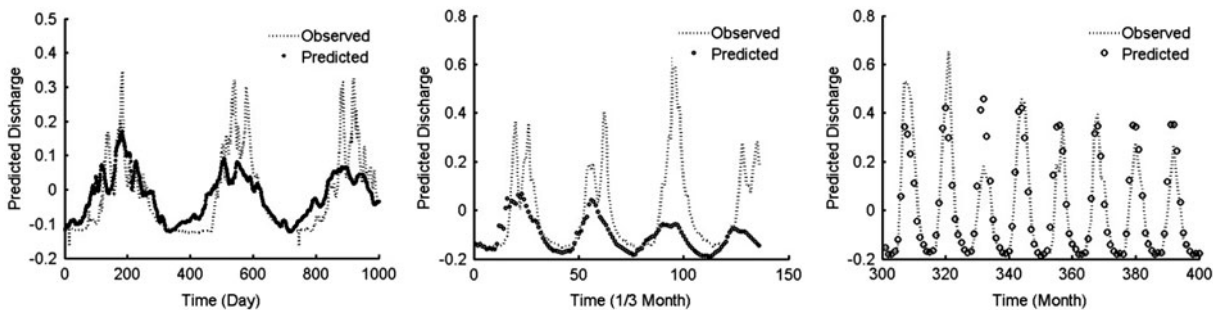

Fig. 8. Prediction performance; left: daily runoff series; right: 1/3 monthly runoff series; and lower: monthly runoff series.
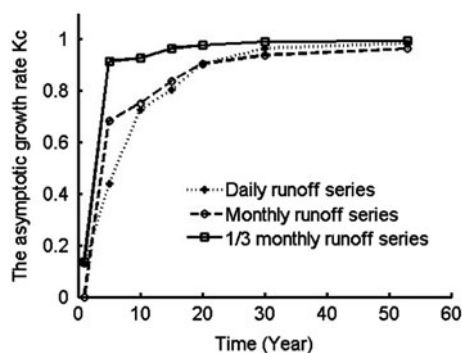
Fig. 9. The asymptotic growth rate at different length and timescales of data.

Table 2
Identification index of chaos characteristics at different timescales

Identification index	Daily	1/3 month	month
Embedding dimension	8	6	5
Delay time	96	13	5
Correlation dimension	3.9570	5.70	4.35
The largest LE	0.0018	0.0034	0.0077
Asymptotic growth rate	0.9851	0.9946	0.9644

increases with the increase of the length, when sample capacity reach to 30 years, the different time scales of runoff series nonlinear gradually close; when the sample size for 53 years, the asymptotic growth rate close to 1. The timescales variance composes only a small fraction of the nonlinearity underlying these processes. Timescale of runoff series have limited influence on nonlinear. In fact, chaos is the state between cycle and random. For runoff series, the key elements of seasonal factors affect the nonlinear characteristics. Table 2 shows the identification index of chaos characteristics of runoff time series.

4. Conclusion

The significance of accepting runoff processes as nonlinear has been gaining considerable in recent times. However, it is hard to explore the types of non-linearity acting underlying the runoff processes and the intensity of the nonlinearity at different timescales. In the application of chaos theory, some basic physical conditions are ignored, because runoff is in an open channels, the nonlinear characteristics of runoff is likely to stem from the initiation of a combination of reservoir operations, tributary inputs, and saturation of groundwater. This paper studies, possible chaotic behaviors in the runoff dynamics for the data recorded at Pingshan station at three timescales (one day, 1/3 month, and one month). The investigation was based on widely used nonlinear research techniques; (1) average mutual information method to determine the delay time, and phase space reconstruction; (2) using false nearest neighbor algorithm the correlation dimension method to estimate the dimension; (3) using Lyapunov exponent method for the analysis of divergence and convergence; the multi-step Volterra adaptive prediction method on the predictability analysis; and (4) using 0–1 test algorithm for the quantitative analysis of chaos characteristics of sample size and timescale. According to 0–1 chaotic algorithm, the asymptotic growth rate closer to 1 with the increase of the sample size and time scales, which means that runoff series of different timescales maintain the similar nonlinear. Time scales have a little impact on the chaos characteristics as the data-set is enough large. The results from these methods provide convincing indication, cross-verification, and confirmation of the existence of low-dimensional chaotic characteristics. For example, existing clear attractor in the phase space; correlation dimension is fractal dimension. The biggest Lyapunov exponents are positive, short-term prediction results are also found to be good. It is evident from the above results that timescales composes only a limit fraction of the intensity of nonlinear behavior.

Acknowledgments

References

[1] R. Khatibi, B. Sivakumar, M.A. Ghorbani, O. Kisi, K. Kocak, Investigating chaos in river stage and discharge time series, J. Hydrol. 414–415 (2012) 108–117.
[2] B. Sivakumar, Correlation dimension estimation of hydrological series and data size requirement: myth and reality, Hydrol. Sci J. 50(4) (2005) 591–603.
[3] C.T. Dhanya, K.D. Nagesh, Nonlinear ensemble prediction of chaotic daily rainfall, Adv. Water Resour. 33 (2010) 327–347.
[4] L.P. Zhang, J. Xia, X.Y. Song, Similarity model of chaos phase space and its application in mid and long-term hydrologic prediction, Kybernetes 38(10) (2009) 1835–1842.
[5] W. Wang, J.K. Vrijling, P. Gelder, J. Ma, Testing for nonlinearity of streamflow processes at different timescales, J. Hydrol. 322 (2006) 247–268.
[6] G.B Sahoo, S.G. Schladow, J.E. Reuter, Forecasting stream water temperature using regression analysis, artificial neural network, and chaotic non-linear dynamic models, J. Hydrol. 378 (2009) 325–342.
[7] I. Falconer, G.A. Gottwald, I. Melbourne, K. Wormnes, Application of the 0–1 Test for chaos to experimental data, SIAM J. Appl. Dyn. Syst. 6 (2007) 395–402.

[8] G.A. Gottwald, I. Melboume, On the Implementation of the 0–1 Test for Chaos, SIAM J. Appl. Dyn Syst. 8 (2009) 129–145.

[9] K.H. Sun, X. Liu, C.X. Zhu, The 0–1 test algorithm for chaos and its applications, Chin Phys B. 19(11) (2010) 510–517.

[10] C.T. Dhanya, K.D. Nagesh, Multivariate nonlinear ensemble prediction of daily chaotic rainfall with climate inputs, J. Hydrol. 403(3–4) (2011) 292–306.

[11] J. Nan, W. He, Characteristic analysis on morphological evolution of suspended particles in water during dynamic flocculation process, Desalin Water Treat. 41 (2012) 35–44.

[12] F. Takens, Detecting strange attractors in turbulence, Lect. Notes Math. 898 (1981) 366–381.

[13] A.M. Fraser, H.L. Swinney, Independent coordinates for strange attractors from mutual information, Phys. Rev. A 33 (1986) 1134–1140.

[14] M.A. Ghorbani, O. Kisi, M. Aalinezhad, A probe into the chaotic nature of daily stream flow time series by correlation dimension and largest Lyapunov methods, Appl. math. Mod. 34 (2010) 4050–4057.

[15] M.T. Rosenstein, J.J. Collins, C.J. Deluca, A practical method for the calculating largest Lyapunov exponents from small datasets, Phys. D 65 (1993) 117–134.

[16] C.N. Lei, I.C. Lou, H. Un, Song, P. Sun, Turbidity removal improvement for Yangtze River raw water, Desalin. Water Treat. 45 (2012) 215–221.